The International Journal of Advanced Manufacturing Technology (2018) 97:511–518
https://doi.org/10.1007/s00170-018-1953-6

ORIGINAL ARTICLE

Mechanical properties of PLA-based composites for fused deposition modeling technology

S. M. Lebedev[1] · O. S. Gefle[1] · E. T. Amitov[1] · D. V. Zhuravlev[1] · D. Y. Berchuk[1] · E. A. Mikutskiy[1]

Received: 27 December 2017 / Accepted: 22 March 2018 / Published online: 4 April 2018

Abstract
To predict the mechanical behavior of 3D printed products, it is important to understand the composite material properties and the effect that parameters of 3D printing process have on the properties of these materials. The mechanical properties of PLA-based composite materials were studied in this work. The mechanical properties of the hot pressed samples were compared to those of the 3D printed samples. The elongation at break and the yield strength of the samples fabricated by 3D printing are decreased by 15–60% compared to those for the hot pressed samples. It has been found that the mechanical properties of 3D printed samples do not practically depending on the deposition scheme.

Keywords Composite polymer materials · Poly(lactic acid) · Mechanical properties · Fused deposition modeling

1 Introduction

It is well-known that poly(lactic acid) (PLA) possesses higher tensile strength among thermoplastic polymers suitable for the fused deposition modeling (FDM) technology [1–4]. Numerous authors showed variations in mechanical properties for 3D printed samples with a strong tension asymmetry and different deposition angles (raster angles) of filament layers. They studied changing deposition angles such as 0°/90°, + 45°/− 45°, and 0°/+ 45°/90°/− 45° and how the main mechanical properties are affected by this factor.

Song et al. [1] showed that the tensile strength and strain for 3D printed PLA samples along the axial, transverse, and out-of-plane directions are significantly different. The authors reported that the out-of-plane direction was the weakest compared to the axial and transverse ones. Besides, the authors found that the tensile strength and strain for 3D printed PLA samples with different deposition angles are decreased in the order 45°, 0°, and 90°. Ciurana et al. [2] also reported that the samples with deposition angle 45° exhibited the highest compression strength. The compression modulus was practically independent of deposition angles of filament layers. Es-Said et al. [4] studied influence of layer orientation on the tensile properties for 3D printed acrylonitrile butadiene styrene (ABS) samples. They found that the tensile strength for 3D printed samples is increased in the following order + 45°, 90°, + 45°/− 45°, + 45°/0°, and 0°. Meanwhile, Carneiro et al. [5] reported that maximum tensile strength and Young's modulus for 3D printed polypropylene (PP) samples are observed for 0° orientation of filament, while the samples with + 45°/− 45° deposition angles have the worst properties. On the other hand, Tymrak et al. [6] found that the tensile strength, elongation, and Young's modulus for 3D printed PLA samples do not practically changed for two deposition conditions such as 0°/90° and + 45°/− 45°. The deviations of the experimental data for these three parameters do not exceed 3.9% for the tensile strength and strain, and 1.5% for Young's modulus, all other things being equal.

The authors [1–4] conclude that changes in the mechanical properties depending on the deposition angle of filament for 3D printed samples can be conditioned by residual stress induced by the volumetric shrinkage of materials at cooling, weak bonding between adjacent filament layers or high level of porosity.

Dielectric properties of PLA do not allow this polymer to be used as an electrically conductive and thermally conductive material in different electrical and thermal devices. Besides, consumer properties of neat PLA limit its use as a material for 3D printed products which should look metallic after additional treatment or have other color shades different from the color

✉ S. M. Lebedev
lsm70@mail.ru

[1] National Research Tomsk Polytechnic University, 2A Lenin Avenue, 634028 Tomsk, Russia

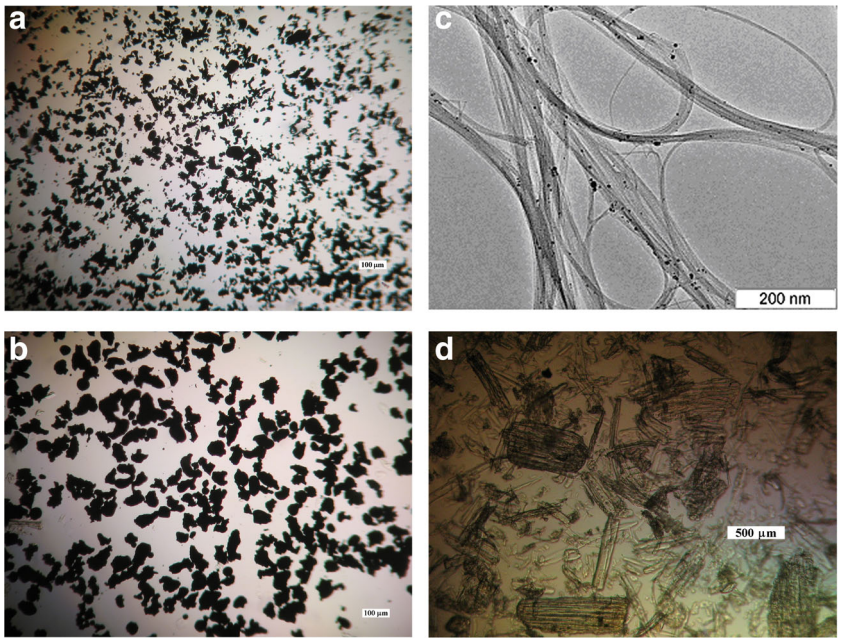

Fig. 1 Photographs of fillers. **a** Bronze powder. **b** Cu powder. **c** CNT bundles. **d** Wood flour

of the neat PLA. It is very important for design of numerous products fabricated by FDM technology by small business owners, allowing them to fabricate customized products for personal use and sale. The absence of commercially available PLA-based composites restricts the wider application of the FDM technology. PLA-based composites are becoming popular due to their new properties which are not inherent to the PLA matrix. Nowadays, different fillers including carbon nanotubes, carbon black, graphene, metal powders, wood flour, etc. are being incorporated into the PLA [7–16]. Carbonaceous fillers and metal powders allow the electric and thermal properties of PLA-based composites to be improved. Organic fillers such as wood flour or cellulose fibers have drawn attention due to their availability, low specific gravity, renewable nature, and biodegradability.

Numerous authors investigated the electric and thermal properties of PLA-based composites [7, 10, 14–16], but mechanical properties of these composites are poorly understood. In our recent paper [7], we have discussed in detail the research results of the electric and thermal properties of PLA-based composites for additive manufacturing. Brief literature review shows that studies of mechanical properties of PLA-based composites filled with different organic or inorganic fillers are very limited. Therefore, the aim of this work was to estimate main mechanical properties of 3D printed samples in comparison with hot pressed ones fabricated of PLA-based composites.

2 Experimental

Biodegradable poly(lactic acid) (PLA, Ingeo 4043D, NatureWorks LLC) was used as a polymer matrix in this work. Powder of metals such as bronze and copper, wood

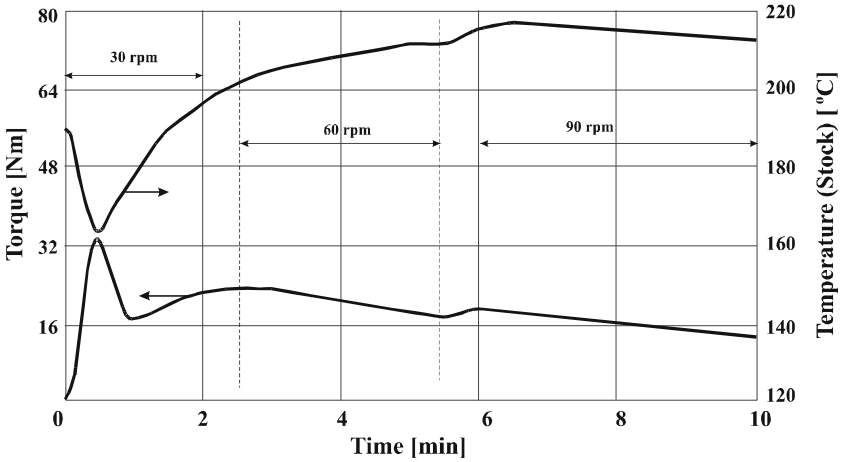

Fig. 2 Typical temporal diagrams of the melt temperature and torque for PLA + 30 wt% bronze

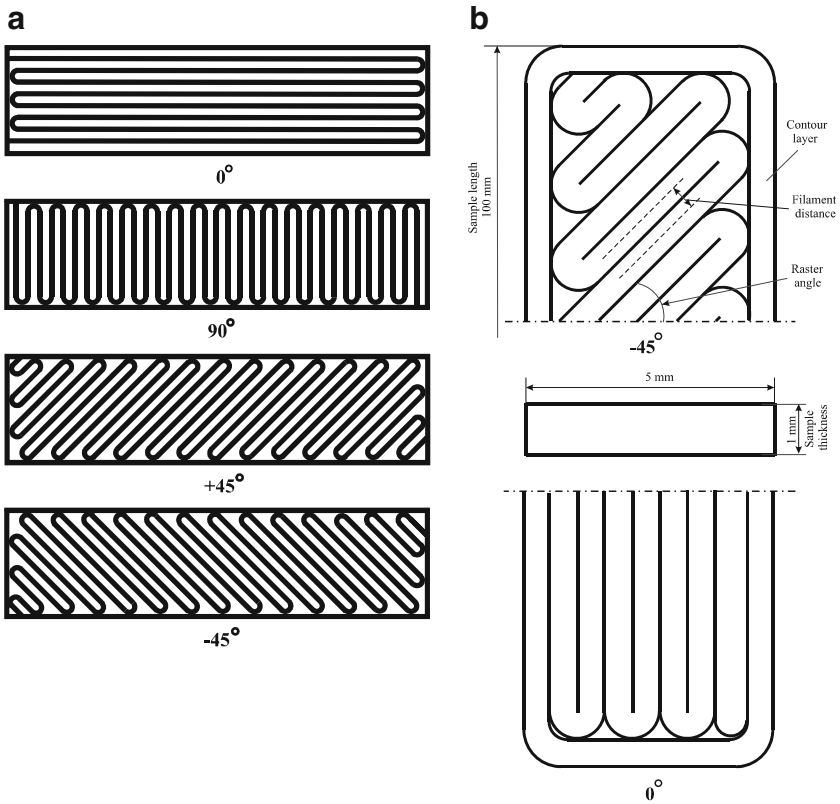

Fig. 3 Schemes of layer deposition for the 3D printed samples

flour, and pristine single-walled carbon nanotubes (CNTs) were used as fillers (Fig. 1). All materials were used "as received" without an additional treatment. The filler content (*C*) in polymer composites was changed from 0 wt% to 30 wt%.

All composites were prepared by mixing in a measuring mixer 50 EHT (Brabender). The processing temperature and mixing time were 190°C and 10 min. The speed of counter-rotating blades of the mixer was changed from 30 rpm to 90 rpm as shown in Fig. 2. Filler was gradually introduced into the polymer melt up to the required fraction, while mixing until all fillers were evenly distributed in the PLA matrix. After preparation, all composites were granulated with the granulator (Brabender).

Large-scale production of PLA-based composites for the filament fabrication was performed by using twin-screw extruder KETSE 20/40D (Brabender). The extruder is equipped with two feed hoppers, the first one (the main feeding) for the polymer matrix material and the second one (the side feeding) for the filler. Temperature profile for six zones of the extruder was adopted 170/180/190/195/190/190 °C, and screw speed for composites filled with wood flour and CNTs was 70 rpm while for composites filled with metal powders, it was set to 50 rpm. PLA-based composite filaments 1.75 mm in diameter for 3D printing were produced using a single-screw extruder. In this case, temperature profile for four zones was 170/190/195/190 °C.

In preparing samples by the hot pressing method, compression molds filled with polymer composite pellets were placed into a vacuum furnace heated to 190 °C for 3 h. After that, compression molds were pressed in a hydraulic press at

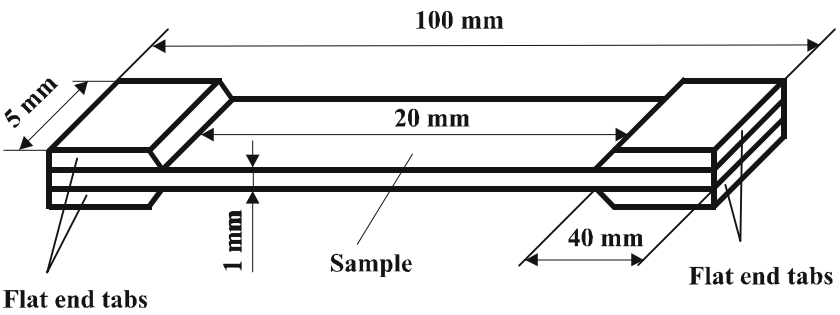

Fig. 4 Sample for tensile tests

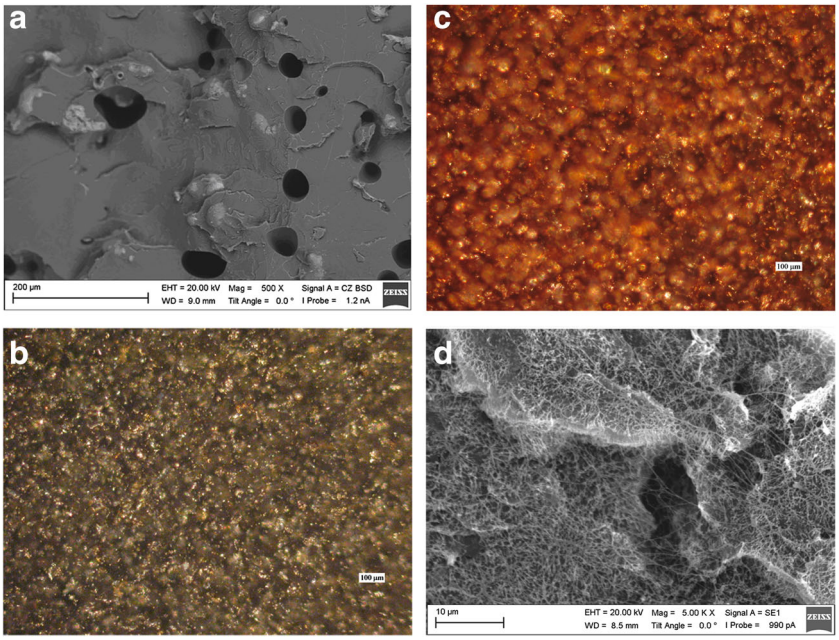

Fig. 5 Photographs of PLA-based composites. **a** SEM micrograph of PLA + 10 wt% bronze. **b** PLA + 30 wt% bronze. **c** PLA + 30 wt% Cu. **d** SEM micrograph of PLA + 0.5 wt% CNT

15 MPa for 20 min. Then, the compression molds were slowly cooled at a cooling rate of 4 °C min^{-1} to ambient temperature under pressure in air.

In preparing the samples and completed products by FDM technology, the Inspire S200 3D printer was used. 3D printer consists of an extruder with a 0.4-mm nozzle diameter positioned at a computer-controlled platform and a working chamber with a lower bed. The temperatures of the extruder head and the heated bed were set to 220 and 60 °C, respectively. 3D printing parameters included printing speed set to 55 mm/s, infill degree of 100%, and filament distance of 0.64 mm. The layer thickness that is responsible for the geometrical resolution was set to 0.25 mm (corresponding to 62.5% of the nozzle diameter). 3D printed PLA samples were prepared by depositing layer-by-layer in accordance with two schemes 0°/90° and + 45°/− 45°, where 0° is the axial direction (along the sample length), and 90° means the transversal direction (Fig. 3). The printing process began with the formation of the external contour layer, which defines finished dimensions of the samples or parts. The next printing stage includes the stacking of the filaments inside the contour layer in accordance with one of the schemes shown in Fig. 3 (e.g., 0° or + 45°). After forming the second contour filament layer, the second inner layer was stacked with raster angle of 90° or − 45°. Consecutive filament layers were stacked layer-by-layer in a similar manner according to the selected scheme.

The contour layer is needed for maintaining particular dimensions of samples because without them, the molten filament material will be deformed due to the volume shrinkage at cooling resulting in variation in the final sample sizes.

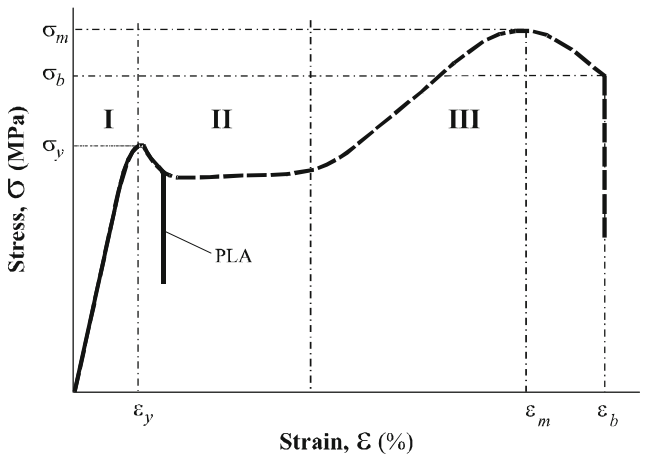

Fig. 6 Typical stress-strain curve for thermoplastic polymers

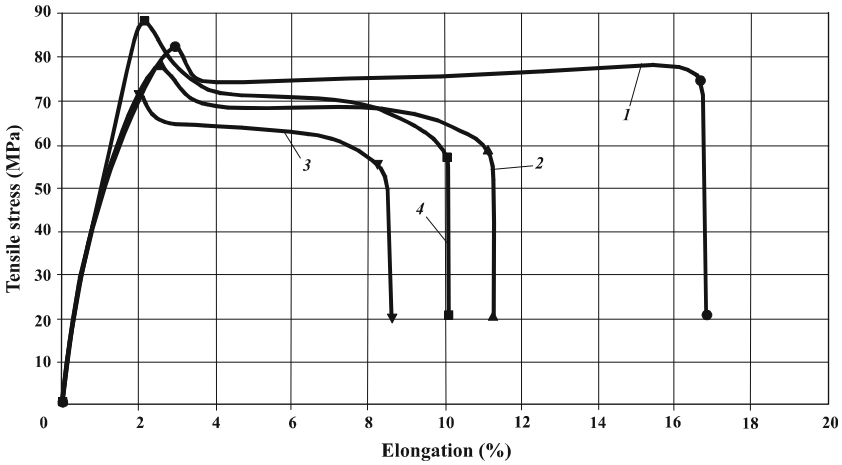

Fig. 7 Stress-strain curves for samples prepared by the hot pressing method: 1, neat PLA; 2, PLA + 30 wt% bronze; 3, PLA + 10 wt% wood flour; 4, PLA + 0.5 wt% CNT

Furthermore, mechanical properties of "a contour free" samples are sharply decreased due to a poor adhesion of filaments at the outside boundary of samples.

The stress-strain curves for samples of neat PLA and PLA composites were measured using an Instron 3345 universal testing machine with a 5-kN load cell at room temperature. The initial distance between grips was 10 mm. The crosshead rate was 10 mm/min. Young's modulus (E), the yield strength (σ_y), and the elongation at break (ε_b) were determined from the stress-strain curves. The samples for tensile tests were prepared as rectangular 100 × 5 × 1 mm plates. Special flat end tabs were placed on the ends of the sample on two opposite sides as shown in Fig. 4. Samples that fractured outside the working area were replaced by new ones. Dimensions of each sample were measured separately before the measurement. The mechanical properties of the hot pressed PLA-based samples were compared to those of the 3D printed ones. At least ten measurements were carried out for all composites and the average values with standard deviations of these parameters were compared.

The morphology of developed composites, shape, and dimensions of fillers were studied by scanning electron microscopy (SEM) and an optical microscopy (OM). Before the study, the samples were fractured in liquid nitrogen. For SEM study, the fracture surface of the samples was covered with silver. When studying the fracture surface of the samples by OM, the tests were carried out in the reflected light without covering the sample surface with silver. Micrographs of fractured surface of the samples prepared of PLA-based composites are shown in Fig. 5. It can be seen that fillers are well-dispersed in the volume of polymer matrix, and no aggregates or agglomerates of filler particles were observed.

3 Experimental results and discussion

Figure 6 shows typical stress-strain curve for thermoplastic polymers. As a rule, the stress-strain curve has the form of a curve with three zones. At the first zone (I), the elongation is proportional to the stress (Hooke's law) until yield point (σ_y, ε_y). Then, necking is observed, after which the elongation increases at the quasi-constant value of the stress (zone II). At this zone, the strain hardening of sample material is observed. At the last zone (III), the further loading leads to breaking the sample.

For PLA-based composites, this process differs considerably (Fig. 7) compared with previous case of ductile polymers. In the vicinity of a yield point, negligible necking continued until the brittle fracture of the sample without visible strain hardening.

3.1 Effect of the filler content

Table 1 represents the tensile test results for neat PLA and PLA-based composites at different filler contents for samples

Table 1 The experimental results of tensile tests for the hot pressed samples

Mechanical properties	Material						
	PLA	PLA + 10% bronze	PLA + 20% bronze	PLA + 30% bronze	PLA + 30% Cu	PLA + 10% wood flour	PLA + 0.5% CNT
ε_b, %	16.7 ± 0.34	16.8 ± 0.4	12.1 ± 0.3	11.1 ± 0.27	13.5 ± 0.3	8.4 ± 0.2	10.0 ± 0.2
σ_y, MPa	83.24 ± 3.7	72.6 ± 4.0	74.6 ± 4.5	77.4 ± 3.5	76.6 ± 4.2	71.0 ± 3.6	87.0 ± 2.6
E, MPa	1100 ± 149	1615 ± 130	1922 ± 170	1885 ± 175	1865 ± 205	1963 ± 200	2012 ± 150

prepared by the hot pressing method. As expected, mechanical properties of PLA-based composites are very sensitive to the filler content. Results obtained demonstrated that adding fillers into PLA matrix results in increase of Young's modulus and decrease of the elongation and the yield strength. It is evident that the elongation at break is not changed for the PLA/bronze composites at the bronze content 10 wt% compared to that for neat PLA. Further increasing the filler content decreases the elongation at break and yield strength of composites by 33.5 and 7%, respectively, at the bronze content of 30 wt% compared with unfilled PLA. On the other hand, Young's modulus is increased (Table 1) and reached 1885 MPa at 30 wt% bronze, which was increased by about 71.4% compared with neat PLA. Drop in the elongation at break and the yield strength of PLA-based composites can be attributed to the availability of filler particles acted as stress concentrators and the poor adhesion between phases. The increase in Young's modulus of PLA-based composites compared with PLA matrix can be caused by the restriction of the polymer chain mobility and deformability due to the presence of filler particles [12, 13]. It can be seen in Table 1 that Young's modulus for PLA-based composites increases about by 70–83% compared with neat PLA, regardless of the filler type, and remained practically unchangeable for all composites taking into account the standard deviations except for the PLA + 10 wt% bronze composite. Lowest value of Young's modulus for the PLA + 10% bronze composite is apparently caused by the fact that the filler content in this case is below "the mechanical percolation threshold." That is, rigid filler network or continuous filler cluster is not formed. Slight increase in Young's moduli for PLA/CNT and PLA/wood flour composites compared to those for PLA-based composites appears to be due to the high aspect ratio of these fillers.

The mean values and standard deviations of mechanical properties for the 3D printed samples prepared of PLA and PLA-based composites are listed in Table 2. As shown in Tables 1 and 2, the hot pressed samples possess substantially higher values of the elongation at break and yield strength than the 3D printed samples, while Young's moduli for 3D printed samples prepared of the neat PLA with deposition angles 0°/90° and 45°/45° are 1744 MPa and 1483 MPa, which are 58.5 and 34.8% higher compared to those of the hot pressed PLA samples. For PLA-based composites, Young's moduli both for the hot pressed samples and the 3D printed ones are practically the same taking into account the standard deviations. Under identical test conditions, the elongation at break and the yield strength of the samples fabricated by 3D printing show a decrease of about 15–60% depending on the deposition scheme and filler type compared to those for the hot pressed samples (see Tables 1 and 2). As mentioned earlier, this may be attributed to such factors as a high porosity, poor adhesion between filament layers, and the formation of voids (poor

Table 2 The experimental results of tensile tests for the 3D printed samples

Mechanical properties	Material						
	PLA	PLA + 10% bronze	PLA + 20% bronze	PLA + 30% bronze	PLA + 30% Cu	PLA + 10% wood flour	PLA + 0.5% CNT
ε_b, %	7.7 ± 0.4/10.4 ± 1.0*	7.5 ± 0.8/8.0 ± 0.6*	6.3 ± 0.9/7.1 ± 0.9*	6.3 ± 0.3/6.7 ± 0.4*	9.3 ± 0.1/9.3 ± 0.2*	6.1 ± 0.1/5.9 ± 0.1*	9.0 ± 0.3/8.9 ± 0.4*
σ_y, MPa	62.4 ± 7.0/71.9 ± 1.2*	55.2 ± 5,3/62.6 ± 2.9*	56.5 ± 5.4/55.7 ± 3.9*	50.0 ± 3.4/56.9 ± 2.3*	64.1 ± 4.2/61.0 ± 3.4*	53.7 ± 3.6/52.1 ± 5.2*	80.0 ± 3.5/79.3 ± 3.7*
E, MPa	1744 ± 149/1483 ± 263*	1765 ± 116/1729 ± 108*	1791 ± 158/1576 ± 199*	1691 ± 191/1969 ± 187*	1769 ± 203/1765 ± 116*	1955 ± 196/1873 ± 138*	1990 ± 170/1870 ± 192*

*(For deposition scheme 0°/90°)/(for deposition scheme + 45°/− 45°)

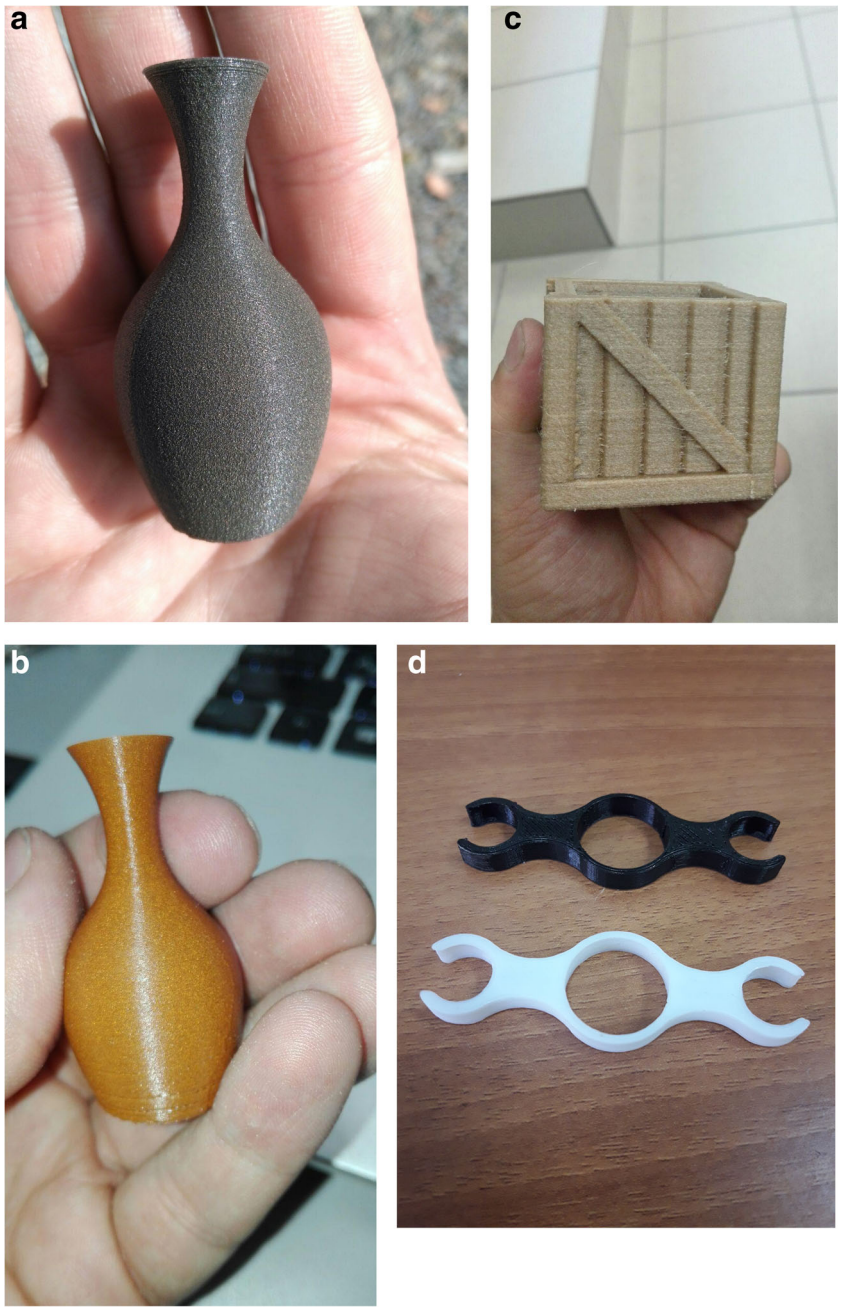

Fig. 8 3D printed products made of PLA-based composites: thin-walled hollow structures: **a** PLA + 50% stainless steel. **b** PLA + 30% Cu; thick-walled structures: **c** PLA + 10% wood flour. **d** PLA and PLA + 30% carbon black

compaction of filament layers) in spite of the 100% infill degree during printing.

3.2 Effect of the deposition angle

It can be seen in Table 2 that the results obtained for two deposition schemes do not practically differ taking into account the standard deviations. This can be attributed to the fact that all 3D printed samples included a contour layer which affected their mechanical properties. Therefore, layers with deposition angles + 45°/− 45° and 0°/90° were not free of this factor and the part of the force applied to the sample was redistributed to the contour layer as this layer has an orientation of 0° (an axial direction coinciding with the applied force direction). Similar effect has been found earlier by Song et al. [1] and Carneiro et al. [5] for unfilled PLA and PP samples.

3.3 Application of developed PLA-based composites for FDM technology

Several examples of 3D printed model structures are shown in Fig. 8 demonstrating that it was possible to fabricate by 3D printing with developed PLA-based composites. On developing 3D printing regimes, for each composite, optimal

processing conditions were defined, such as temperature of head and a working chamber, printing velocity, cooling regime, infill degree, layer thickness, and permissible deviations of the filament diameter. It was found that developed PLA-based composites can be used for printing not only thick-walled structures but also thin-walled hollow structures of required quality without deformation and defects. Furthermore, developed PLA-based composites with required properties may be processed by extrusion or injection molding.

4 Conclusions

The mechanical properties of neat PLA and PLA-based composites were studied in this work. We have demonstrated that developed composites containing different fillers such as metal powders, wood flour, and CNTs are suitable for the FDM technology. We have also shown the preparation of composites, the filament extrusion, 3D printed and hot pressed PLA-based samples for mechanical tests, and 3D printed model structures. Comparative tensile tests have shown that developed PLA-based composites can be applied to produce end-used products fabricated by FDM technology in spite of some deterioration in mechanical properties compared to the similar products manufactured by conventional techniques such as injection molding or hot pressing. Besides, PLA-based composites with desired properties allow expanding the nomenclature of polymer composite materials suitable for FDM technology.

Funding information The authors gratefully acknowledge financial support for this work from the National Research Tomsk Polytechnic University (project TPU CEP-IPHT-73/2017).

Compliance with ethical standards

Conflict of interest The authors declare that they have no conflict of interest.

References

1. Song Y, Li Y, Song W, Yee K, Lee K-Y, Tagarielli VL (2017) Measurements of the mechanical response of unidirectional 3D-printed PLA. Mater Des 123:154–164
2. Ciurana J, Serenóa L, Vallèsa E (2013) Selecting process parameters in RepRap additive manufacturing system for PLA scaffolds manufacture. Procedia CIRP 5:152–157
3. Matsuzaki R, Ueda M, Namiki M, Jeong T-K, Asahara H, Horiguchi K, Nakamura T, Todoroki A, Hirano Y (2016) Three-dimensional printing of continuous-fiber composites by in-nozzle impregnation. Sci Rep 6:23058. https://doi.org/10.1038/srep23058
4. Es-Said OS, Foyos J, Noorani R, Mendelson M, Marloth R, Pregger BA (2000) Effect of layer orientation on mechanical properties of rapid prototyped samples. Mater Manuf Process 15(1): 107–122
5. Carneiro OS, Silva AF, Gomes R (2015) Fused deposition modeling with polypropylene. Mater Des 83:768–776
6. Tymrak BM, Kreiger M, Pearce JM (2014) Mechanical properties of components fabricated with open-source 3-D printers under realistic environmental conditions. Mater Des 58:242–246
7. Lebedev SM, Gefle OS, Amitov ET, Berchuk DY, Zhuravlev DV (2017) Poly(lactic acid)-based polymer composites with high electric and thermal conductivity and their characterization. Polym Test 58:241–248
8. Tekce HS, Kumlutas D, Tavman IH (2007) Effect of particle shape on thermal conductivity of copper reinforced polymer composites. J Reinf Plast Compos 26(1):113–121
9. Lebedev SM, Gefle OS, Amitov ET, Berchuk DY, Zhuravlev DV (2017) Influence of heavy metal powders on rheological properties of poly(lactic acid). Russ Phys J 60(4):624–630
10. Laureto J, Tomasi J, King JA, Pearce JM (2017) Thermal properties of 3-D printed polylactic acid-metal composites. Prog Addit Manuf 2:57–71
11. Chieng BW, Ibrahim NA, Then YY, Loo YY (2016) Mechanical, thermal, and morphology properties of poly(lactic acid) plasticized with poly(ethylene glycol) and epoxidized palm oil hybrid plasticizer. Polym Eng Sci 56:1169–1174
12. Zakaria Z, Islam MS, Hassan A, Haafiz MKM, Arjmandi R, Inuwa IM et al (2013) Mechanical properties and morphological characterization of PLA/chitosan/epoxidized natural rubber composites. Adv Mater Sci Eng 2013:629092. https://doi.org/10.1155/2013/629092
13. Pilla S, Gong S, O'Neill E, Rowell RM, Krzysik AM (2008) Polylactide-pine wood flour composites. Polym Eng Sci 48:578–587
14. Xue B, Ye J, Zhang J (2015) Highly conductive poly(L-lactic acid) composites obtained via in situ expansion of graphite. J Polym Res 22(112). https://doi.org/10.1007/s10965-015-0755-x
15. Lizundia E, Oleaga A, Salazar A, Sarasua JR (2012) Nano- and microstructural effects on thermal properties of poly(L-lactide)/multi-wall carbon nanotube composites. Polymer 53:2412–2421
16. Sullivan EM, Gerhardt RA, Wang B, Kalaitzidou K (2016) Effect of compounding method and processing conditions on the electrical response of exfoliated graphite nanoplatelet/polylactic acid nanocomposite films. J Mater Sci 51:2980–2990